Acta Crystallographica Section D
**Biological Crystallography**
ISSN 0907-4449

# Purification and crystallization of the heterodimeric complex of RAR$\beta$ and RXR$\alpha$ ligand-binding domains in the active conformation

**Vivian Pogenberg, Jean-François Guichou and William Bourguet***

Centre de Biochimie Structurale, CNRS UMR 5048–Inserm U554, Faculté de Pharmacie, 15 Avenue Charles Flahault, 34093 Montpellier, France

Correspondence e-mail: bourguet@cbs.cnrs.fr

Received 31 March 2004
Accepted 23 April 2004

The ligand-binding domains of the retinoid X receptor $\alpha$ (RXR$\alpha$) and of the retinoic acid receptor $\beta$ (RAR$\beta$) were overexpressed separately and copurified in the heterodimeric form. Using a crystallization solution containing sodium formate and PEG 3350 as precipitant, the heterodimer was cocrystallized with the promiscuous ligand 9-*cis*-retinoic acid (9C-RA) and a 13-residue fragment of the nuclear receptor interaction domain (NID) of the transcriptional coactivator TRAP220. The crystals grew in the trigonal space group $P3_121$, with unit-cell parameters $a = b = 115.7$, $c = 247.2$ Å and two heterodimers per asymmetric unit. X-ray diffraction data were collected to 2.9 Å resolution. The structure was solved by molecular replacement and is currently being refined.

## 1. Introduction

Retinoic acid receptors (RAR$\alpha$, $\beta$ and $\gamma$) and retinoid X receptors (RXR$\alpha$, $\beta$ and $\gamma$) are ligand-activated transcription factors that belong to the superfamily of nuclear receptors (NRs). They transduce the pleiotropic effects of retinoic acids on cell differentiation, proliferation and apoptosis (Ross *et al.*, 2000; Altucci & Gronemeyer, 2001; Bastien & Rochette-Egly, 2004). Whereas RARs bind and are activated by either the 9-*cis* or all-*trans* isomers of the retinoic acid, RXRs are exclusively activated by the 9-*cis* isomer. Like other NRs, RARs and RXRs share a common functional and structural organization, with six regions commonly labelled from A to F with evolutionary conserved DNA (DBD, region C) and ligand (LBD, region E) binding domains. The LBD also harbours a ligand-dependant activation function termed AF-2, a repression function and a strong dimerization surface. The remaining domains are much less conserved and consist of the N-terminal A/B region containing a ligand-independent transactivation function (AF-1), the short D region that appears to correspond to a flexible hinge between the highly structured C and E domains and finally the C-terminal F region for which no clear function has been assigned (Germain *et al.*, 2003; Bastien & Rochette-Egly, 2004). To date, only the DBDs and LBDs of several NRs have been described at the structural level (Renaud & Moras, 2000).

Various crystallographic structures of unliganded (apo), agonist-bound (holo) or antagonist-bound NR LBDs have revealed a common model for the regulation of AF-2 by the ligands (Bourguet, Germain *et al.*, 2000; Renaud & Moras, 2000). The binding of an agonist ligand to an NR triggers a mechanism by which the most C-terminal LBD helix H12 is repositioned in such a way that it generates a surface required for coactivator association. In contrast, binding of an antagonist prevents the formation of this surface. The ligand-induced recruitment of coactivators to NRs is mainly mediated by a short L*xx*LL helical motif present in the NR interaction domain (NID) of the coactivators (McKenna & O'Malley, 2002). Some NRs may act as monomers or homodimers, but many of them, for example RAR, the vitamin D receptor (VDR) and the peroxysome proliferator-activated receptor (PPAR), are functionally active on their cognate response element as a heterodimeric association with the promiscuous heterodimerization partner RXR. In the context of the heterodimer, both RAR and RXR protomers can bind their ligand. Recently, the crystal structure of a heterodimeric complex of RAR$\alpha$ and RXR$\alpha$ LBDs in a fully antagonistic conformation was solved, revealing the ligand-induced allosteric events that account for the transcription characteristics of partial agonistic and antagonistic retinoid ligands (Bourguet, Vivat *et al.*, 2000). In order to better characterize the interaction between RAR/RXR heterodimers and transcriptional coregulators, we solved the crystal structure of the heterodimer comprising the fragments RXR$\alpha$ E and RAR$\beta$ EF. Both LBDs are complexed with one 9C-RA molecule and one L*xx*LL motif-containing peptide derived from the NID of the transcriptional coactivator TRAP220. This structure reveals the agonist conformation for RAR$\beta$ and RXR$\alpha$ in a heterodimeric context and comparison with previously determined structures of RAR and RXR LBDs in various oligomeric and liganded forms could help to

gain insight into the structure–function relationships of the heterodimers. Notably, the determination of the structure of the F region in the context of a heterodimer could provide information about its possible functional role. Here, we describe the expression, purification and the preliminary steps of structure determination of the complex.

## 2. Experimental procedure and results

### 2.1. Protein expression and purification

The histidine-tagged LBD of mouse RAR$\beta$ (residues 146–448 in a pET15b vector) and the LBD of mouse RXR$\alpha$ (residues 226–467 in a pET3a vector) were expressed in *Escherichia coli* BL21(DE3). Cells were grown at 310 K in LB medium supplemented with 100 µg ml$^{-1}$ ampicillin until $OD_{600}$ reached about 0.6. Expression of T7 polymerase was induced by addition of isopropyl-$\beta$-D-thiogalactoside (IPTG) to a final concentration of 0.5 m*M*. After an additional incubation for 3 h at 298 K, cell cultures were harvested by centrifugation at 8000*g* for 15 min. The cell pellets from 2 l of RXR$\alpha$ and 4 l of RAR$\beta$ LBDs were mixed and resuspended in 75 ml buffer *A* (20 m*M* Tris–HCl pH 8, 500 m*M* NaCl, 5 m*M* imidazole). Lysozyme was added to 200 µg ml$^{-1}$. After 30 min on ice, the suspension was lysed by sonication and centrifuged at 90 000*g* at 277 K for 30 min. The supernatant was loaded onto a 5 ml $Ni^{2+}$-affinity column (HiTrap chelating column, Amersham Biosciences) equilibrated with buffer *A* using the Äkta purifier system (Amersham Biosciences). The column was washed with 20 volumes of buffer *A* and 20 volumes of 50 m*M* imidazole in buffer *A*. Bound proteins were eluted with buffer *A* containing 150 m*M* imidazole. The fractions containing the eluted proteins were pooled, dialysed against buffer *B* (10 m*M* Tris–HCl pH 7.5, 150 m*M* NaCl, 5 m*M* DTT) and incubated overnight with a twofold molar excess of 9C-RA (ICN) and thrombin (Sigma). The protein was further purified using a Superdex 75 26/60 gel-filtration column (Amersham Biosciences) calibrated with globular standard proteins (gel-filtration calibration kit, Amersham Biosciences) and pre-equilibrated with buffer *B*. The purity of the fractions was analysed by SDS–PAGE. The fractions eluting at the expected size for the heterodimer and containing equal amounts of pure RXR$\alpha$ and RAR$\beta$ were pooled, concentrated and mixed with a twofold molar excess of 9C-RA and a threefold molar excess of TRAP220-NR2 peptide (641-NHPMLMNLLKDNPA-654). The heterodimer was more than 95% pure as judged from the Coomassie-stained gels (Fig. 1).

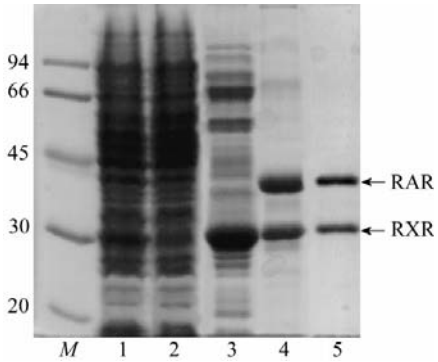


**Figure 1**
Purification of the RAR$\beta$–RXR$\alpha$ heterodimer. Representative Coomassie-stained 12.5% SDS–PAGE of pools from protein purification. Lane *M*, molecular-weight markers (in kDa); lane 1, soluble protein crude extract; lane 2, flowthrough from the $Ni^{2+}$-charged HiTrap chelating column; lane 3, wash collection from the HiTrap column showing a large excess of RXR$\alpha$ not retained on the column; lane 4, pool of the heterodimer eluted from the HiTrap column (after thrombin cleavage); lane 5, purified heterodimer after gel filtration.

### 2.2. Crystallization

The purified protein was concentrated to approximately 15 mg ml$^{-1}$ and centrifuged for 30 min at 20 800*g* prior to crystallization assays. Crystallization trials were performed by hanging-drop vapour diffusion at 291 K using 24-well plates (Nextal, Canada). Hampton Research Crystal Screens and the NR-LDB screen (Molecular Dimensions Ltd) were used to determine the initial crystallization conditions. The protein solution was mixed with an equal volume of the reservoir solution to give a final volume of 4 µl and placed on the cover slips. The wells contained 500 µl reservoir solution. Several conditions containing polyethylene glycol (PEG) produced small crystals. The best heterodimer crystals were observed using condition No. 21 of the PEG/Ion Screen (Hampton Research). This condition was further refined to produce larger crystals and a single crystal was finally obtained in a condition containing 100 m*M* sodium formate and 20% PEG 3350. The crystal grew in 4 d to final dimensions of 0.45 × 0.25 × 0.25 mm and was bipyramidal in shape with a hexagonal base (Fig. 2).

### 2.3. Data collection and processing

The protein crystal was mounted from the mother liquor onto a cryoloop (Hampton Research), sequentially soaked in the reservoir solution containing an additional 5–25% glycerol in five steps (5, 10, 15, 20 and 25%) and finally quickly frozen in liquid nitrogen. Diffraction data were collected at 100 K using a MAR CCD (165 mm) detector at the French Beamline for Investigation of Proteins (BM30A) at ESRF (Grenoble, France). The crystal was rotated through 120° with an oscillation angle of 0.5° per frame and an exposure time of 30 s per image. Diffraction data were processed using *MOSFLM* (Leslie, 1992) and scaled with *SCALA* from the *CCP*4 program suite (Collaborative Computational Project, Number 4, 1994). Data-collection statistics are given in Table 1. The crystal belongs to space group $P3_121$, with two dimers in the asymmetric unit and a solvent content of 65.5%. The structure was solved by molecular replacement using the *MOLREP* software (Vagin & Teplyakov, 1997) from the *CCP*4 suite with a truncated version of the RAR$\alpha$–RXR$\alpha$ heterodimer (Bourguet, Vivat *et al.*, 2000) as the search model. In this model, all water and ligand molecules were removed as well as the RAR$\alpha$ and RXR$\alpha$ C-terminal helices H12, which were expected to adopt different conformations in the two dimers. Two solutions were

**Table 1**
Data-collection details and statistics.

Values in parentheses refer to the highest resolution shell (3.06–2.9 Å).

| | |
|---|---|
| Wavelength (Å) | 0.9797 |
| Space group | $P3_121$ |
| Unit-cell parameters (Å) | $a = b = 115.7$, $c = 247.2$ |
| Matthews coefficient (Å$^3$ Da$^{-1}$) | 3.6 |
| Solvent content (%) | 65.5 |
| No. observations | 317475 |
| No. unique reflections | 43014 |
| Redundancy | 7.4 (7.5) |
| $R_{sym}$† | 0.083 (0.383) |
| Completeness (%) | 99.7 (99.6) |
| $I/\sigma(I)$ | 5.2 (2.0) |

† $R_{sym} = \sum|I_i - \langle I\rangle|/\sum I_i$, where $I_i$ is the mean intensity of symmetry-related measurements of the reflections.

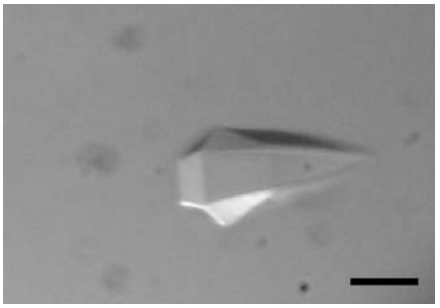

**Figure 2**
Crystal of the RAR$\beta$–RXR$\alpha$ heterodimer. Crystal dimensions are 450 × 250 × 250 µm. The scale bar corresponds to approximately 200 µm.

obtained from the molecular-replacement search with a correlation coefficient of 0.269 (next highest solution 0.189) and an *R* factor of 0.575, consistent with the presence of two complexes in the asymmetric unit. The final solution comprising two heterodimers had a correlation coefficient of 0.472 (next highest solution 0.240) and an *R* factor of 0.492. The presence of a clear electron density for the two molecules of 9C-RA confirmed the molecular-replacement solution. Moreover, the presence of continuous electron densities for the two helices H12 in the expected agonist position, for the two coactivator peptides and for some residues of the F region of RAR$\beta$ became apparent at the early stages of the structure refinement. The refined structure of the complex will be published elsewhere.

We acknowledge experimental assistance from the staff of the FIP beamline at the ESRF in Grenoble during data collection. This work was supported by funds from the INSERM, CNRS and Université Montpellier I (UMI). VP was the recipient of a grant from the Réseau National des Génopoles, Ministère de la Recherche.

## References

Altucci, L. & Gronemeyer, H. (2001). *Trends Endocrinol. Metab.* **12**, 460–468.
Bastien, J. & Rochette-Egly, C. (2004). *Gene*, **328**, 1–16.
Bourguet, W., Germain, P. & Gronemeyer, H. (2000). *Trends Pharmacol. Sci.* **21**, 381–388.
Bourguet, W., Vivat, V., Wurtz, J. M., Chambon, P., Gronemeyer, H. & Moras, D. (2000). *Mol. Cell*, **5**, 289–298.
Collaborative Computational Project, Number 4 (1994). *Acta Cryst.* D**50**, 760–763.
Germain, P., Altucci, L., Bourguet, W., Rochette-Egly, C. & Gronemeyer, H. (2003). *Pure Appl. Chem.* **75**, 1619–1664.
Leslie, A. G. W. (1992). *Jnt CCP4/ESF–EACBM Newsl. Protein Crystallogr.* **26**, 27–33.
McKenna, N. J. & O'Malley, B. W. (2002). *Cell*, **108**, 465–474.
Renaud, J. P. & Moras, D. (2000). *Cell. Mol. Life Sci.* **57**, 1748–1769.
Ross, S. A., McCaffery, P. J., Drager, U. C. & De Luca, L. M. (2000). *Physiol. Rev.* **80**, 1021–1054.
Vagin, A. & Teplyakov, A. (1997). *J. Appl. Cryst.* **30**, 1022–1027.